

Firefly Luciferin-activated Rose Bengal: *In Vitro* Photodynamic Therapy by Intracellular Chemiluminescence in Transgenic NIH 3T3 Cells¹

Theodossis Theodossiou,^{2,3} John S. Hothersall,^{2,3} Elizabeth A. Woods, Klaus Okkenhaug, Jake Jacobson, and Alexander J. MacRobert

National Medical Laser Centre, Department of Surgery, University College London, W1W 7EJ London, United Kingdom [T. T., A. J. M.]; Department of Urology and Nephrology, University College London, London W1W 7EJ, United Kingdom [J. S. H.]; Ludwig Institute for Cancer Research, London W1W 7BS, United Kingdom [E. A. W., K. O.]; and Department of Molecular Pathogenesis, Institute of Neurology, London WC1N 3BG, United Kingdom [J. J.]

ABSTRACT

Photodynamic therapy (PDT) of cancer (1, 2) is a well-established treatment modality that uses light excitation of a photosensitive substance to produce oxygen-related cytotoxic intermediates, such as singlet oxygen or free radicals (3, 4). Although PDT is advantageous over other forms of cancer treatments because of its limited side effects, its main disadvantage is the poor accessibility of light to more deeply lying malignancies. External light sources such as lasers or lamps can be applied either noninvasively to reach tumors that lie well within the penetration depth of the light or in a minimally invasive fashion (interstitial treatments) in which optical fibers are placed intratumorally through needles. Even with the second approach, light distribution over the tumor is not homogeneous and nonidentified metastatic disease is left untreated. CL, the chemical production of light, is exemplified by firefly light emission mediated by the enzymatic (luciferase + ATP) oxidation of D-luciferin to oxyluciferin (5). This mobile light source is a targetable alternative to external sources of illumination. Here we show the *in vitro* photodynamic effect of rose bengal activated by intracellular generation of light, in luciferase-transfected NIH 3T3 murine fibroblasts.

INTRODUCTION

The use of CL⁴ for the excitation of a photosensitizer (hypericin) has been used for the *in vitro* inactivation of the equine infectious anemia virus (6). Coincubation in medium with hypericin, D-luciferin, luciferase, and ATP induced a 10-fold decrease in the viral infectivity at high hypericin and luciferase concentrations.

We propose that D-luciferin and a photosensitizer when taken up by luciferase-transfected cells, as a consequence of their intracellular proximity, produce sufficient light to release singlet oxygen by photoactivation and to trigger individual cell death.

Two possible mechanisms of excitation of the photosensitive molecule exist within that reference frame: radiative absorption of CL emission and direct energy transfer (of a Förster type) from oxyluciferin to the photosensitizer. For efficient direct energy transfer, a close proximity (<10 nm) of the oxyluciferin and the photoactive molecules is required (6). For this reason, the chemical characteristics of the chosen photosensitizer are of key importance. Firstly, the photosensitizer should have an absorption profile that closely matches the emission profile of oxyluciferin; secondly, it should have a high quantum yield of singlet oxygen when activated; and, lastly, it should locate in the same cellular compartment as D-luciferin, luciferase, and

ATP. A photosensitizer that meets these criteria is the water-soluble xanthene dye, RB with a high singlet-oxygen quantum yield of $\Phi_{\Delta} \approx 0.75$, as reported in the literature (7).

MATERIALS AND METHODS

D-Luciferin CL Spectrum. Light emission from 100 μ l of D-luciferin-luciferase solution (Labsystems ATP monitoring kit) in 2 ml PBS after the addition of 10 μ M ATP was scanned in a Perkin-Elmer spectrofluorimeter (LS5) using a CL attachment. The emission profile was recorded by the tuning of the emission monochromator with no excitation light. Subsequently, RB (5 nM) was added, and a new emission profile was obtained.

RB Absorption Spectrum. The absorption profile of RB (10 nM) in 1 ml of PBS was recorded in a CARY 1E Varian spectrophotometer. The background absorption profile of PBS was subtracted to yield the absorption spectrum of RB.

Cell Transfection and Culture. NIH 3T3 cells were grown in DMEM supplemented with 10% FCS and 100 units/ml penicillin-streptomycin (Invitrogen) at 37°C in 5% CO₂. At 60–70% confluence, the cells were transfected with plasmid DNA by using the Qiagen Superfect method with a total of 12 μ g of DNA per 10-cm culture dish. The DNA mixture consisted of 10 μ g of the Promega PGL3-control vector that contained cDNA encoding the modified firefly luciferase under the control of the SV40 promoter and a gene that confers ampicillin resistance. The other 2 μ g of DNA was the pIRES neomycin resistance expression vector (CloneTech) for the rapid identification of the transfected cells by antibiotic selection. The cultures were grown for 48 h, and the cells were passaged at 1:10 and 1:20 into their normal growth media plus G418 disulphate (1 mg/ml, Melford Laboratories) until colonies appeared. The individual colonies were then transferred to culture dishes and were maintained under their normal growth conditions plus G418 until confluent when one-half were transferred to a flask and one-half were harvested and assayed using the Promega luciferase assay system.

Confocal Microscopy. NIH 3T3-luc+ cells were inoculated and grown on 25-mm glass coverslips in 35-mm dishes (10⁵ cells/dish) and were left overnight. Cells were then incubated in serum-free medium with RB (10 μ M) for 3 h. The coverslips were then placed over the $\times 40$ oil immersion, quartz objective (NA 1.3) of a Zeiss 510 CLSM confocal microscope, in physiological saline, and the cells were excited using the 543-nm line of a HeNe laser (1% of total laser power). The fluorescence was collected at wavelengths longer than 585 nm.

D-luciferin (Promega) subcellular localization was imaged by the same system after the *in situ* addition of 500 μ M D-luciferin in 10% FCS medium. The fluorescence of luciferin was excited using the 351-nm laser line (3% total) and the image was obtained beyond 505 nm.

RB-Uptake Studies. NIH 3T3-luc+ murine fibroblasts were inoculated (10⁴/well) and incubated with RB (10 μ M) in medium \pm 1% FCS for 0–6 h. After incubation, cells were washed twice with PBS and fluorescence was measured in a Galaxy FLUORstar spectrofluorimeter, equipped with a 96-well plate reader to monitor intracellular RB fluorescence. The excitation wavelength was 550 nm, and the emission was 590 nm.

CL Measurements in Cells. CL measurements on NIH 3T3-luc+ cells, were made in a chemiluminometer incorporating a light-tight, rotating, measurement head thermostated at 37°C. The sample was rotated above a +5-cm lens and under a concave mirror. The active window of a Hamamatsu (R943–02) photon-counting PMT was situated underneath the lens at its focal point. The quantum efficiency of the PMT was 15% at the peak of oxyluciferin emission. The signal from the PMT was fed to an optimized amplifier-

Received 12/19/02; accepted 2/14/03.

The costs of publication of this article were defrayed in part by the payment of page charges. This article must therefore be hereby marked *advertisement* in accordance with 18 U.S.C. Section 1734 solely to indicate this fact.

¹ J. S. H. was supported by The St. Peters Trust, E. A. W. was supported by Biotechnology and Biological Sciences Research Council, K. O. was supported by a European Union Framework V grant, and J. J. was supported by the Medical Research Council.

² T. T. and J. S. H. contributed equally to the work.

³ To whom requests for reprints should be addressed, at University College London, Charles Bell House, 67–73 Riding House Street, W1W 7EJ London, United Kingdom. E-mail: t.theodossiou@ucl.ac.uk or j.hothersall@ucl.ac.uk.

⁴ The abbreviations used are: CL, chemiluminescence; RB, rose bengal; MTT, 3-(4,5-dimethylthiazol-2-yl)-2,5-diphenyltetrazolium bromide; FCCP, carbonyl cyanide *p*-trifluoromethoxy-phenylhydrazone; PDT, photodynamic therapy; PMT, photomultiplier tube.

discriminator system and, subsequently to a Thorn Electron Tubes photon-counting card, interfaced to a personal computer for data acquisition and storage.

CL-PDT Experiments. Cells (10^4 /well) were plated in a 96-well plate and were used the following day. Cells, when appropriate, were treated with RB in serum-free media for 3 h. Control groups were treated in an identical fashion without RB. A D-luciferin and RB-lycopene control group was included as well as a non-PDT-RB group. After this time, cells were washed once in serum-containing medium and then were incubated for 24 h in the same medium in the presence or absence of $500 \mu\text{M}$ D-luciferin. Lycopene (Sigma; $5 \mu\text{M}$), when used, was added at this time. Particular attention was paid to the exclusion of all ambient light throughout the incubation, and all of the manipulations were carried out under a dimmed red light to avoid the activation of RB.

MTT Assay. MTT assays were performed to determine the cell survival rate. Each well was incubated with medium containing MTT (1 mg/ml) for 3 h. The medium was then removed and $100 \mu\text{l}$ of DMSO (Sigma) were added per well. After 20 min at room temperature with agitation, samples were read in a microplate reader (Titertek Multiskan MCC), using a 540-nm filter.

RESULTS AND DISCUSSION

Initially the spectral compatibility of the absorption profile of RB with the CL emission of luciferase/ATP-catalyzed oxyluciferin was assessed. The emission spectrum of oxyluciferin CL was recorded (Fig. 1, dotted line), together with the absorption spectrum of RB (Fig. 1, solid line). Excellent compatibility between the two was observed. The RB addition (Fig. 1b, curve 2) altered the spectral profile of D-luciferin-luciferase/ATP-induced CL (Fig. 1b, curve 1). The difference spectrum of curves 2 and 1 (Fig. 1b, curve 3) indicates a strong attenuation of the oxyluciferin emission at the spectral region of RB absorption.

To further test our hypothesis, NIH 3T3 murine fibroblasts, transfected with the modified luciferase gene (*Luc+*, cytosolic expression),

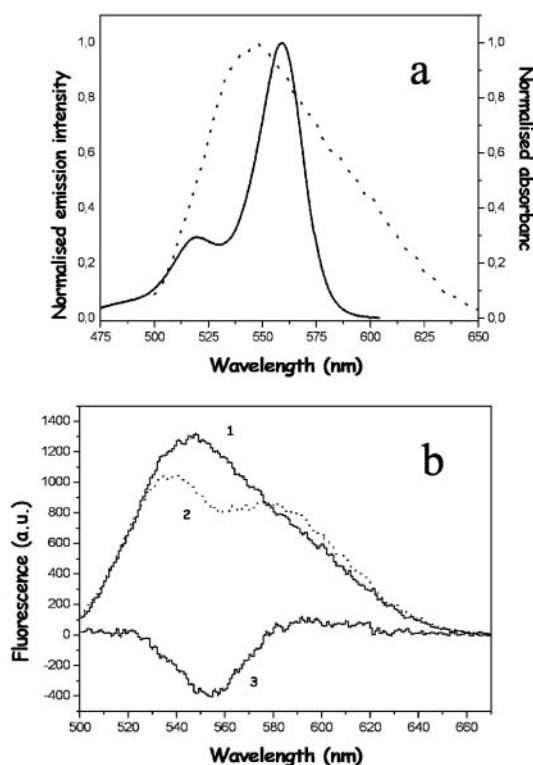


Fig. 1. Compatibility of RB absorption with Luciferase/ATP oxyluciferin emission. *a*, the emission profile of D-Luciferin oxidized by firefly luciferase and ATP (dotted line) and the absorption profile of RB (10 nM). *b*, the emission spectrum of oxyluciferin (curve 1 solid), the modified emission, after the addition of RB (10 nM; curve 2) and their difference spectrum (curve 3).

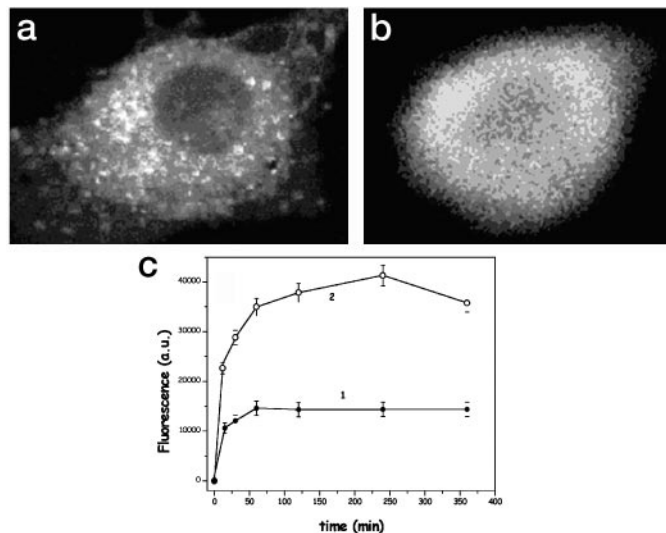


Fig. 2. RB and D-Luciferin cellular uptake. *a*, a confocal fluorescence image of a NIH 3T3-Luc+ cell after a 3-h incubation with $10 \mu\text{M}$ RB in serum-free medium. Excitation was at 543 nm, and the fluorescence was collected after a 585-nm-long pass filter. *b*, a confocal fluorescence image of a NIH 3T3-Luc+ cell directly after the addition of $500 \mu\text{M}$ D-luciferin in 10% FCS-containing medium. The excitation was at 351 nm, and the fluorescence was collected after a 505-nm-long pass filter. *c*, RB uptake time course as monitored by fluorescence. NIH 3T3 cells were incubated with $10 \mu\text{M}$ RB for up to 6 h in 10% FCS-containing medium (curve 1) and FCS-free medium (curve 2). The fluorescence was excited at 550 nm and monitored at 590 nm by a Galaxy Fluorstar spectrofluorimeter.

were used as a model. Transfection with the *Luc+* gene led to efficient expression of luciferase within the NIH 3T3-luc+ cells (as detailed in "Materials and Methods").

The uptake and subcellular distribution of RB in NIH 3T3-luc+ cells was imaged using confocal microscopy (Fig. 2a) and revealed a predominantly diffuse cytosolic distribution, with some staining of the nuclear membrane and spherical organelles.

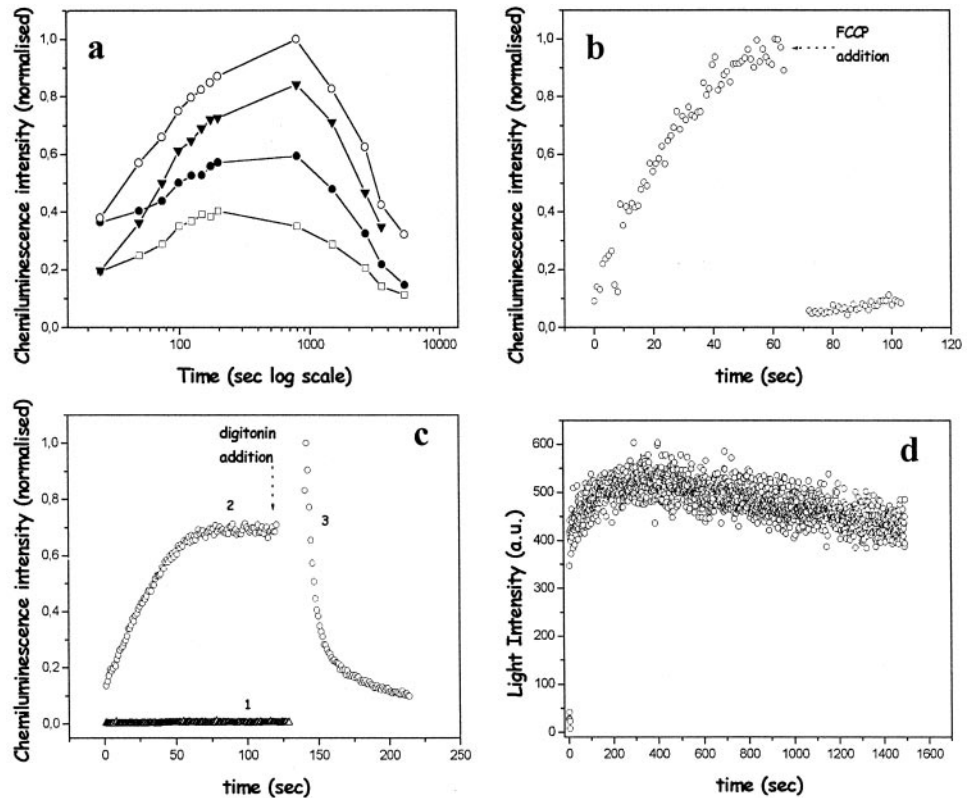
Likewise, the uptake and subcellular localization of D-luciferin was imaged in NIH 3T3-luc+ cells after the subtraction of cell autofluorescence (Fig. 2b). Again, a diffuse cytosolic distribution of D-luciferin within the cells was observed.

The time-dependent uptake of RB by NIH 3T3-luc+ cells was measured as the increasing fluorescence emission in intact cells incubated in medium both with and without FCS. The time course of fluorescence (uptake profile) that was obtained appears in Fig. 2c. It is clear from this graph that incubation in serum-free medium (curve 2) enhanced the uptake of RB. This was not caused by changes in RB fluorescence in FCS, because in cell-free conditions, RB, in either FCS-free or 1% FCS media, yielded the same fluorescence intensity (data not shown). Three hour incubation yielded optimal RB uptake. The cells incubated with RB in serum-free medium were subsequently lysed by the addition of Triton X-100, and a higher fluorescence signal was observed in the supernatant. Further addition of 0.5 N perchloric acid to precipitate protein, followed by centrifugation ($10,000 \times g \text{ min}^{-1}$) abolished the fluorescence signal, indicating that RB was associated with cellular proteins (data not shown). Calibration of RB fluorescence in the supernatant after cell lysis yielded a value of $\sim 5 \times 10^9$ molecules of RB internalized per cell after the 3-h incubation.

The efficiency of luciferase transfection was assessed in intact NIH 3T3-luc+ cells by measuring CL after the addition of D-luciferin.

Both the intensity and the duration of the CL activity induced at different concentrations of D-luciferin were measured. Dishes containing 10^5 cells were incubated with 170, 340, 500, and $670 \mu\text{M}$ D-luciferin in 10% FCS-containing medium. The resultant CL time

Fig. 3. CL in luciferase-transfected NIH 3T3-Luc+ cells. *a*, CL duration and intensity measurements in cells incubated with 170 (\square), 340 (\bullet), 500 (\circ) and 670 (\blacktriangle) μM D-luciferin. *b*, verification of the absolute requirement of intracellular ATP using the mitochondrial uncoupler FCCP (2 μM). *c*, addition of 500 μM D-luciferin to medium removed from cells (*curve 1*); effects of cell permeabilization on steady state CL after the addition of digitonin (4 μM ; *curves 2 and 3*). *d*, CL profile of NIH 3T3 cells before PDT experiments.



course (Fig. 3*a*) showed that, although the profile of the CL was the same at all concentrations, the peak of CL intensity increased up to 500 μM (\circ) followed by a decrease at 670 μM (\blacktriangle). This cannot be attributed to ATP depletion, because CL is not enhanced at any point; however, it may result from chemical toxicity at this concentration. An optimal concentration of D-luciferin of 500 μM was chosen.

In parallel experiments performed when CL had reached a steady state, the protonophore FCCP (2 μM) was added to uncouple mitochondria and deplete intracellular ATP. Within seconds of the addition of FCCP, luminescence dropped to background levels, clearly showing that luciferase-D-luciferin oxidation was dependent on intracellular ATP (Fig. 3*b*). The intracellular nature of the CL was confirmed by showing that media taken from cells incubated for 24 h, together with D-luciferin and 10 μM ATP, produced no light (Fig. 3*c*, *curve 1*) and that 10 μM ATP, added to cells producing steady-state CL did not enhance the light signal (data not shown). However, when digitonin (4 μM) was used to permeabilize the cells after they had reached steady-state CL, an immediate and marked enhancement in light was observed (Fig. 3*c*, *curve 3*). In this instance, as the cell membranes were permeabilized, D-luciferin from the medium freely entered the intracellular space resulting in the observed rapid increase in CL intensity. However, after progressive membrane rupture, intracellular luciferase and ATP were released and diluted in the medium; and, because ADP rephosphorylation could not occur, there was a rapid decrease of CL intensity to background levels (Fig. 3*c*, *curve 3*). This confirmed the exclusively intracellular nature of luciferase and the fact that, in intact cells, it was not the limiting factor for the CL emission.

Cells were seeded in 96-well plates (10^4 /well) and left 24 h to equilibrate. At the same time, 10^5 cells were plated into 35-mm dishes and CL was measured after the addition of 500 μM D-luciferin (Fig. 3*d*). From the steady-state light emission, it was calculated that ~ 60 photons/cell/s were produced. This value corresponds to an approximate light-fluence rate of ~ 1 mW/ μm^2 at the boundary of the cellular

membrane and to 10 atto units of luciferase per cell, because approximately one photon is produced for every oxidized luciferin molecule (5). At the same time, this also equates to the possible intracellular generation of 45 singlet oxygen molecules/cell/s.

In additional experiments, cells were treated with RB (10 μM) for 3 h in FCS-free media. Control cell groups (no additions and D-luciferin alone) were subjected to identical treatment without RB. Throughout this and all of the subsequent treatments, ambient light was totally excluded. After treatment, all of the groups were washed once in medium with 10% FCS and then were incubated in the same medium either without (control) or with 500 μM D-luciferin (PDT). The cells were left for 24 h, and then cell survival was assessed by MTT. The control groups (Fig. 4, *columns 1, 2, 3, and 4*) all exhibited 100% survival within experimental error. However, cells treated with both RB and D-luciferin (PDT group, Fig. 4, *column 5*) exhibited an arresting 90% toxicity, which can be attributed only to the phototoxicity of RB, activated by intracellular CL. Moreover, the respective cells that were cotreated with lycopene, a potent singlet oxygen

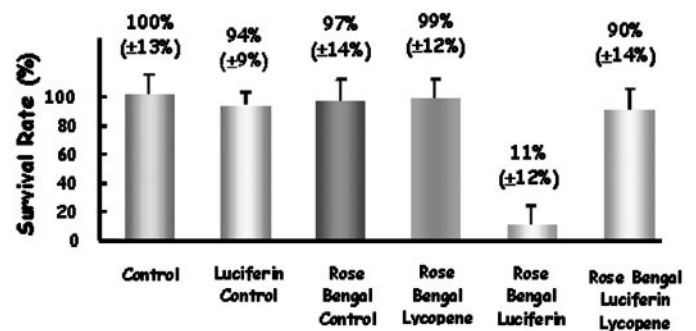


Fig. 4. Photocytotoxicity of RB activated by intracellular CL in NIH 3T3-Luc+ cells as shown by MTT assay. RB (10 μM for 3 h)-treated cells subjected to 24-h D-luciferin (500 μM)-light activation (*column 5*). Antioxidant effects of Lycopene (*column 6*).

quencher (8) exhibited 90% survival (Fig. 4, column 6), implying that the phototoxicity is mainly a result of singlet-oxygen production.

These *in vitro* results suggest new prospects for the application of targeted PDT *in vivo*: CL-PDT.

One possibility is the use of liposomes prepared with selected ligand antibodies (9) targeted to specific cancer cells for the delivery of the CL components together with the photosensitizer. After fusion of the liposomes with target cell membranes and content internalization, intracellular ATP would initiate the CL production and, thus, photosensitizer activation.

Another possible mode of instigating intracellular PDT would be via *in vivo* transfection of the target cells with the luciferase gene, via appropriate viral vectors and consequent systemic or intratumoral application of D-luciferin and the photosensitizer. Recent work on *in vivo* luciferase imaging by Adams *et al.* (10) has shown the immediate feasibility of this prospect by demonstrating the ability to image and identify metastasis in a human-prostate cancer model using a prostate-specific adenovirus vector carrying the luciferase gene and a charge-coupled device imaging system. The engineered, prostate-specific promoter, linked to the luciferase gene, facilitated expression of the gene only in cells that expressed prostate-specific antigen. Our data, for the first time, demonstrate cytotoxicity through the production of intracellular light and introduce the possibility of targeting this light specifically to tumor cells for a potent and plausible modality for certain cancer treatments.

ACKNOWLEDGMENTS

We thank Amir Ahmed for valuable help; Bart Vanhaesebroeck, Michael Duchon, and Alberto Dutra for their support and constructive criticism; and M. P. Gordge for critical reading of the manuscript.

REFERENCES

1. Dougherty, T. J. Photodynamic therapy. *Photochem. Photobiol.*, 58: 895–900, 1993.
2. Hopper, C. Photodynamic therapy: a clinical reality in the treatment of cancer. *Lancet Oncol.*, 1: 212–219, 2000.
3. Ochsner, M. Photophysical and photobiological processes in the photodynamic therapy of tumours. *J. Photochem. Photobiol. B Biol.*, 39: 1–18, 1997.
4. Fuchs, J., and Thiele, J. The role of oxygen in cutaneous photodynamic therapy *Free Radicals. Biol. Med.*, 24: 835–847, 1998.
5. McElroy, W. D., and DeLuca, M. *Bioluminescence and Chemiluminescence*, pp. 179–186. New York: Academic Press, 1981.
6. Carpenter, S., Fehr, M. J., Kraus, G. A., and Petrich, J. W. Chemiluminescent activation of the antiviral activity of hypericin: a molecular flashlight. *Proc. Natl. Acad. Sci. USA*, 91: 12273–12277, 1994.
7. Redmond, R. W., and Gamlin, J. N. A compilation of singlet oxygen yields from biologically relevant molecules. *Photochem. Photobiol.*, 70: 391–475, 1999.
8. Di Mascio, P., Kaiser, S., and Sies, H. Lycopene as the most efficient biological carotenoid singlet oxygen quencher. *Arch. Biochem. Biophys.*, 274: 532–538, 1989.
9. Koning, G. A., Kamps, J. A., and Scherphof, G. L. Efficient intracellular delivery of 5-fluorodeoxyuridine into colon cancer cells by targeted immunoliposomes. *Cancer Detect. Prev.*, 26: 299–307, 2002.
10. Adams, J. Y., Johnson, M., Sato, M., Berger, F., Gambhir, S. S., Carey, M., Iruela-Arispe, M. L., and Wu, L. Visualisation of advanced human prostate cancer lesions in living mice by a targeted gene transfer vector and optical imaging. *Nat. Med.*, 8: 891–896, 2002.